

## Magnetotelluric exploration of the Gross Schönebeck low enthalpy geothermal reservoir

Gerard Muñoz, Oliver Ritter, Inga Moeck

German Research Centre for Geosciences, Telegrafenberg, 14473 Potsdam, Germany

gmunoz@gfz-potsdam.de

**Keywords:** Magnetotellurics, Electrical conductivity, 2D Inversion, Low enthalpy geothermal system, Northeast German basin

### ABSTRACT

Electrical conductivity is a key parameter for the exploration and characterization of geothermal reservoirs as (hot) mineralized formation water of (active) geothermal areas usually exhibits significantly higher electrical conductivity than the surrounding host rock. In this work we present results of a magnetotelluric (MT) exploration experiment carried out in the vicinity of the Groß Schönebeck (Germany) geothermal test site, where a doublet system has been drilled to establish an *in situ* laboratory to investigate the potential for geothermal energy production. The MT data were recorded along a 40-km long main profile, centred on the doublet, and a 20-km long parallel profile, located 3 km to the east. Classical two-dimensional smooth inversion of the MT data reveals a shallow conductive layer which delineates an antiform-like shape above a Permian thick evaporitic layer. This result is consistent with information from regional geology and seismic images. However, at the northermost part of the profiles, the conductivity models resolve deep reaching conductive structures which appear uncorrelated with existing (geophysical or geological) data. Incorporating seismic and well data as independent constraints for the 2D inversions of the MT data allows us to examine the model space rigorously but target-oriented, introducing a certain degree of subjectivity. Employing so-called *tear zone* inversions we can effectively derive an alternative class of models, which are consistent with the MT observations but also with the additional information. We speculate that the zones of high conductivity imaged at the level of the reservoir at approximately 4-5 km depth are related to salt lows (areas of reduced salt thickness) of the overlaying evaporite layer. The enhanced conductivity of these regions can be explained by higher porosity (fracture density) in anhydritic areas and/or generally lower resistivity of the pore fluid.

### 1. INTRODUCTION

The EU funded project I-GET (Integrated Geophysical Exploration Technologies for Deep Fractured Geothermal Systems) is aimed at developing innovative strategies for geophysical exploration of geothermal deep water systems in different geological contexts. These include high enthalpy reservoirs, such as the volcanic rocks in Hengill, Iceland or the magmatic and metamorphic geological setting in Travale, Italy and also, low enthalpy, deep sedimentary basins such as in Groß Schönebeck, Germany and Skiernewice, Poland. The basic idea is to integrate all available knowledge, from geology, rock physics to seismic and magnetotelluric (MT) deep sounding.

The Groß Schönebeck deep sedimentary reservoir is representative for large sedimentary basins which exist all over Europe. The Groß Schönebeck test site consist of a doublet made up of the wells GrSk 3/90 and GrSk 4/05, and is currently used as an *in situ* geothermal laboratory. To ensure high enough productivity for geothermal exploitation, the detection of permeable zones and fluid bearing fractures at depth is crucial. The magnetotelluric method is a natural-source electromagnetic method capable of imaging the subsurface electrical conductivity down to depths of several kilometres. Since electrical conductivity depends strongly on the presence of fluids, their temperature and salinity, the magnetotelluric method is a very promising exploration technique for geothermal reservoirs.

### 2. MT DATA ACQUISITION AND PROCESSING

MT data was collected along a 40 km-long main profile centred around the well doublet and a shorter, approximately 20 km-long parallel profile located 3 km to the east (Figure 1). The direction of the profiles was chosen approximately perpendicular to the known strike direction of the geological structures (Figure 1). The main profile consists of 55 stations with a site spacing of 400 m in the central part (close to the borehole) of the profile, increasing to 800 m towards the profile ends. The parallel profile to the east consists of 18 stations with a site spacing of 1 km. The period range of the observations was 0.001 to 1000 s. At all sites, we recorded horizontal electric and magnetic field components and the vertical magnetic field.

Given the amount of electromagnetic noise present in the survey area, approximately 30 km north of Berlin, a long recording time was necessary to improve the statistical properties of the collected data. To further improve the data quality, additional MT stations were set-up to as remote reference sites for the data processing. The remote site delivering the highest quality was setup on the island of Rügen, approximately 200 km to the north of the profile. The geomagnetic and impedance tensor transfer functions were obtained using the robust processing algorithm described in Ritter et al. (1998), Weckmann et al. (2005), and with modifications by Krings (2007) which were developed within the framework of the IGET project. Most of the curves show similar apparent resistivity values of roughly 40  $\Omega$ m at the highest frequencies, indicating that static shift is generally a minor problem. A few curves with higher static shift were manually moved to the common apparent resistivity level. Figure 2 shows an example of the data.

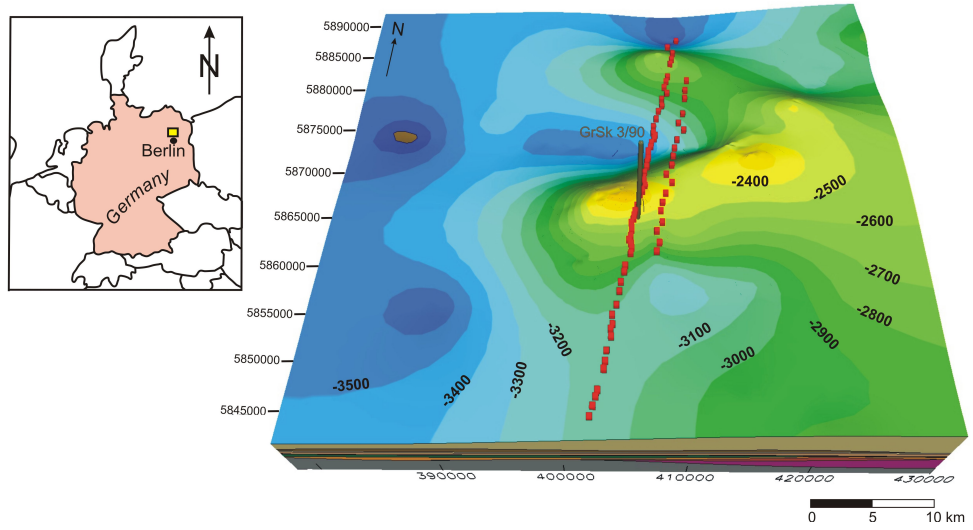


**Figure 1:** Three-dimensional view to the top of the Zechstein with the location of the MT stations (red dots) superimposed. The grey solid line represents the path of the borehole GrSk 3/90. The MT data were acquired in two experiments in summer 2006 and winter 2007. The map of the Zechstein was compiled using existing seismic data, boreholes and regionally geology. Data along the approximately 40 km long main profile (to the left) was gathered along a coincident active seismic experiment

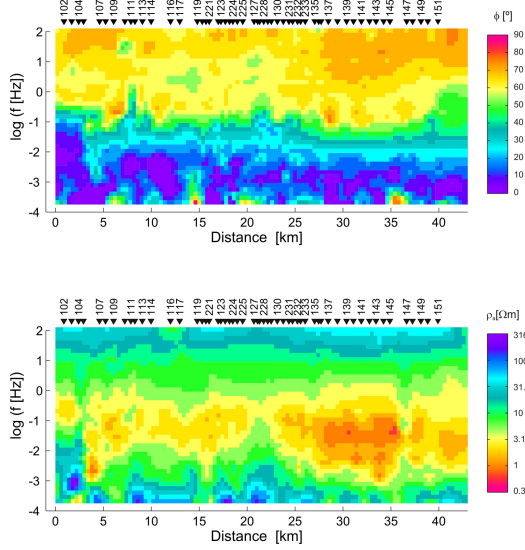


**Figure 2:** Pseudosections of the phase (upper panel) and apparent resistivity (lower panel) of the TE mode data of the main profile

To analyze dimensionality and directionality of the data we used the code of Becken & Burkhardt (2004). This technique examines the impedance tensor in terms of polarization states of the electric and magnetic fields. Analyzing ellipticities of the field polarizations, the regional strike direction can be identified even if galvanic distortion is present. For both profiles, strike directions vary very consistently around 70°W between individual stations, thereby indicating a mainly two-dimensional conductivity structure. This is consistent with a multi-period, multi-site analysis of the regional strike, which also results in a direction of N70W. For the parallel profile, strike directions show a slightly higher dispersion, scattering around 70–80°W; the multi-site, multi-period analysis of the regional

strike direction results in N73W. This means that the MT data are dominated by regional two-dimensional structures and, hence, 2D inversion of the data is appropriate.

### 3. TWO-DIMENSIONAL INVERSION

#### 3.1 Regularized Inversion

Prior to the inversion and according to the dimensionality analysis all data of the main profile were rotated to -70°. The 2D inversion of the MT data was calculated using the algorithm of Rodie & Mackie (2001), which produces a minimum structure model using as a stabilizing functional a simple, second-difference operator which approximates the Laplacian if the grid is uniform. This approach produces smooth models, with gradual changes of resistivity from one cell to the other as strong resistivity contrasts are penalized by the regularization functional. The relative weight of the misfit and the regularization functional is controlled via a trade-off parameter ( $\tau$ ), which has to be chosen for each model. A standard procedure for estimating the optimal  $\tau$  value is the so called L-curve study. Several inversions with different  $\tau$  values are run, and for each of those the RMS misfit (first term of the functional) is plotted against the model roughness (second term); the optimal value for  $\tau$  is found close to the corner-point of the L-curve (i.e. the value which minimises both terms at the same time). For the present work a value of  $\tau=10$  was chosen.

Figure 3 shows the smooth (or minimum structure) models obtained from the inversions of the apparent resistivity and phases of TE and TM modes as well as the vertical magnetic transfer functions using a regularization parameter of  $\tau = 10$  (see above). The models are plotted together with sedimentary horizons from the geological model of Moeck et al. (2008) (Fig. 5). Using error floor settings of 10% for the apparent resistivities, 1.5° for the phases and 0.05 for the geomagnetic transfer functions, RMS misfits of 2.17 and 1.84 were obtained for the main and parallel profiles, respectively.

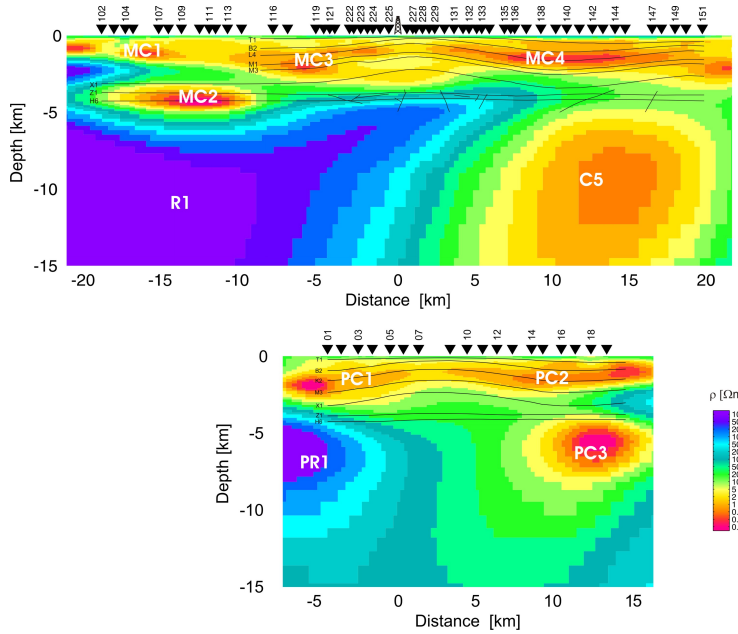


**Figure 3: Resistivity models of both profiles obtained from smooth inversion. The thin black lines represent the stratigraphic horizons obtained from the geological model. C and R labels denote prominent conductive and resistive bodies with M indicating they belong to the main profile and P to the parallel profile; their significance is discussed in the text**

The resistivity model for the main profile (Fig. 3) shows three shallow conductive bodies (C1, C3 and C4) which seem to form a continuous conductive layer extending from surface down to about 2.5 km depth with an antiform-like shape. Towards the southern end of the profile another conductive body (C2) appears beneath the conductive layer, clearly disconnected from C1 and overlying a resistive body (R1) that extends from a depth of about 5 km towards the bottom of the model along the entire southern half of the profile. In contrast, a deep-reaching high conductivity body (C5) occupies most of the northern half of the model, from a depth of about 5 km downwards. The resistivity model obtained from the parallel profile in Fig. 3 shows a very similar result with conductive bodies C1 and C2 forming a shallow conductive layer with antiform shape. The deep-reaching conductive body C3 is related in shape and location to C5 from the main profile and a similar resistive body (R1) appears in the southernmost part of the model.

### 3.2 Tear Zones Inversion

The main MT profile is collocated with a seismic tomography profile (Bauer et al., 2009). The seismic velocity model shows consistently high Vp velocities  $> 5.5$  km/s for depths below 4 km, and a relatively homogeneous, velocity distribution. There are no indications in the Vp model for features that could be related to the deep conductors C5 and C3 in the main and parallel profiles respectively. In fact, the high Vp velocities at depth  $> 4$  km are among the features resolved with greater reliability in the seismic models and they appear to be consistent with the borehole data, which indicate the basin floor at this depth.

To resolve this apparent discrepancy between MT data and the other geo-information we tested whether we could find alternative MT models which are compatible with a resistive basin floor at depths greater than 4 km. To test this hypothesis a number of so called tear zones inversions were carried out. The inversion code of Rodi and Mackie (2001) allows dividing the model space into different regions, so-called tear zones. In these regions the model

norm is minimized independently without interaction between them. Strong resistivity contrasts between tear zones are not penalized by the regularization of the inversion procedure. Tear zones inversions result in a different class of models than those obtained from smooth inversion.

As starting models for the tear zones inversions we used the models obtained by smooth inversion. We divided the models into two tear zones based on the horizon which is thought to represent the top of the Lower Permian volcanic rocks, and thus defines the basin floor. For the starting model, we assigned a homogeneous resistivity of  $100 \Omega\text{m}$  to the zone above the tear boundary and  $1000 \Omega\text{m}$  below, representing a resistive basin floor. An inversion of apparent resistivity, phase and geomagnetic transfer functions was carried out for each profile, applying the same error floors as in the previous cases (10% for the apparent resistivities,  $1.5^\circ$  for the phases and 0.05 for the geomagnetic transfer functions). The RMS misfit of 2.27 for the main profile and 1.85 for the parallel profile are similar to the smooth inversion results. Figure 4 shows the models obtained from the tear-zone inversions.

As expected, the upper 4 km of the models remain essentially the same for both types of inversion (compare Figs. 3 and 4), i.e. the general shape, position and conductivity of C1, C3 and C4 from the main profile and of conductors C1 and C2 from the parallel profile are similar. The strongest difference is found in the deeper part of the profiles, where the conductors C2-C5 and C3-C4 (see main and parallel profiles respectively) are now re-located above the resistive basement, showing much lower resistivity values ( $0.1 \Omega\text{m}$  vs.  $1 \Omega\text{m}$ ) when compared with the smooth inversion models.

Note that the overall RMS misfit alone is not a significant criterion to determine if the two models are equivalent. However, after a close examination of the model responses of each site we conclude that both model classes are equivalent within the data errors.

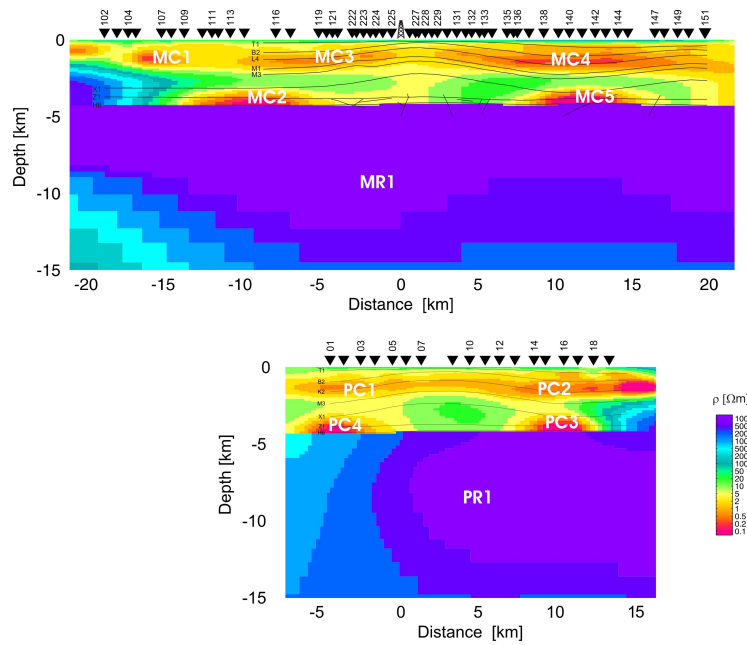


**Figure 4:** Resistivity models of both profiles obtained from tear zones inversion. The model is divided into the two tear zones (see text for details). The thin black lines represent the stratigraphic horizons obtained from the geological model. C and R labels denote prominent conductive and resistive bodies with M indicating they belong to the main profile and P to the parallel profile; their significance is discussed in the text

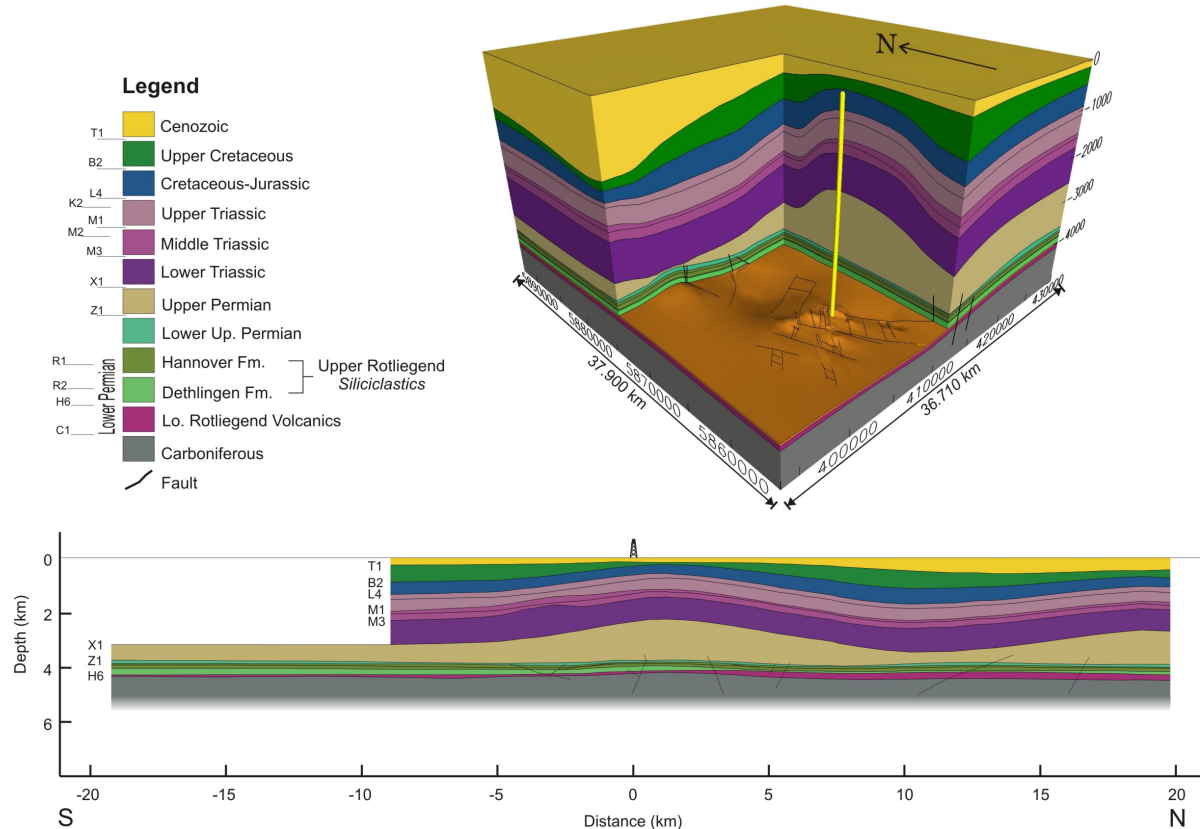


**Figure 5:** Three-dimensional view of the geological model of the study area obtained from refraction seismic lines and borehole data (Moeck et al., 2008) and cross-cut of the model along the main MT profile

## DISCUSSION

At surface, the Tertiary sediments are imaged as a moderately conductive layer ( $20 - 50 \Omega\text{m}$ ) in both profiles. These porous, unconsolidated sediments comprise sands, gravel and clay. The shallow conductive layers (MC1 – MC3 – MC4 of the main profile and PC1 – PC2 of the parallel profile) present an antiform shape and coincide with the Mesozoic sedimentary sequences above the Buntsandstein formation (Cretaceous to Upper Triassic, Fig. 5). This sequence encompasses weak or soft rocks such as clay, marl, marly limestone and some thin layers of limestone and sandstone as revealed by borehole logs. As these materials have significant porosity, they can store significant volumes of fluids, which in turn can lead to increased conductivity. Regions with the highest conductivity within these shallow layers could correspond to the presence of conductive clay minerals and/or very high porous materials like less consolidated sandstones.

As the geometry, depth and conductivity of the deep conductors MC5 in the main profile and PC3 in the parallel profile is not well resolved, their nature is speculative and subject to different interpretations. Following the smooth inversion models (Fig. 3) the conductors are imaged as extended anomalies reaching depths of 15 km and 10 km, respectively. In this case, they could represent deep-reaching fault systems associated with Variscan collision zones

On the other hand, in the tear zones inversion models, the deep conductors (MC2, MC5 in the main profile and PC3, PC4 in the parallel profile) coincide with the Rotliegend level. These conductive bodies occur below the areas where the Zechstein (Upper Permian) salt layer presents local lows, while we observe only moderate resistivities beneath the salt upwelling in the Rotliegend. The deep high conductivity bodies could be caused by fluids, possibly with salinities in excess of 260 g/l (Giese et al., 2001). Based on these salinities, temperatures on the order of 150 °C, and porosities around 15% (Holl et al., 2005) the modelled resistivities of ( $0.1 \Omega\text{m}$  and  $2 \Omega\text{m}$ , respectively) can be explained by Archie's law (Archie, 1942), assuming fracture dominated porosity beneath the salt lows and pore dominated porosity beneath the salt upwelling zones. Higher resistivity regions in the Rotliegend can be interpreted as a lower porosity (fracture density) or generally lower electrical conductivity of the pore fluid. The main lithological unit of the Zechstein lows could be dominated by anhydrite, which shows brittle behaviour under stress and is therefore perceptive for fracturing. In contrast, regions of salt upwelling are caused by plastic deformation which is less susceptible for fracturing.

## CONCLUSIONS

Two different classes of resistivity models were obtained from regularized inversion, with two different regularization approaches. Classical two-dimensional smooth inversion (Figure 3) produces a resistivity cross-section which resolves a shallow conductive layer (3 km depth) delineating an antiform shape above the Permian evaporites (Zechstein). These models, however, reveal deeper structures ( $> 5$  km depth) which do not agree with existing geophysical and geological data. A second class of models is derived using a different regularization approach, the so-called tear zones inversion. This way strong resistivity contrast across the tear zones borders are not penalized. This alternative class of models includes information obtained from seismic tomography (Bauer et al., 2009), i.e. introducing a high resistivity basin floor as a

constraint in the inversion. With the use of tear zones inversion the model space can be explored more rigorously and target oriented.

Both model classes produce consistent images of supra-salt structures but they differ in the deeper parts of the models, i.e. the presence of a resistive basin floor and the shape and location of deeper conductive anomalies.

The target-oriented tear zones inversion (Figure 4) reveals zones of high conductivity related to areas in the reservoir level (Rotliegend), associated with anhydrite-rich salt lows in the overlaying evaporite layer (Zechstein). In this context, we speculate that the enhanced conductivity is associated with fracturing in the brittle anhydrites, resulting in enhanced hydraulic permeability.

## ACKNOWLEDGMENTS

This work was funded within the 6<sup>th</sup> Framework Program of the European Union (IGET Project, Contract n° 518378). The instruments for the magnetotelluric experiments were provided by the Geophysical Instrument Pool Potsdam (GIPP). For their unselfish help in the field, we would like to thank: Michael Becken, Katharina Becker, Jana Beerbaum, Markus Briesemeister, Juliane Hübner, Andre Jung, Frohmut Klöß, Christoph Körber, Thomas Krings, Ansa Lindeque, Naser Meqbel, Carsten Müller, Stefan Rettig, Wladislaw Schafrik, Manfred Schüler, Ariane Siebert, Jacek Stankiewicz, Ute Weckmann and Wenke Wilhelms.

## REFERENCES

Archie, G.: The electrical resistivity log as an aid in determining some reservoir characteristics. *Trans. Am. Inst. Min. Metall. Pet. Eng.*, **146**, (1942), 54–62.

Bauer, K., Schulze, A., Weber, M. and Moeck, I.: Refraction seismic tomography around the geothermal site at Gross Schoenebeck, Northeast German basin. (2009), Submitted.

Becken, M. and Burkhardt, H.: An ellipticity criterion in magnetotelluric tensor analysis. *Geophys. J Int.*, **159**, (2004) 69–82.

Giese, L., Seibt A., Wiersberg T., Zimmer M., Erzinger J., Niedermann S. and Pekdeger A.: Geochemistry of the formation fluids. In: 7. Report der Geothermie Projekte, In situ-Geothermielabor Groß Schönebeck 2000/2001 Bohrarbeiten, Bohrlochmessungen, Hydraulik, Formationsfluide, Tonminerale. (2001), GeoForschungsZentrum Potsdam.

Holl, H.-G., Moeck, I., and Schandlmeier, H.: Characterisation of the tectono-sedimentary evolution of a geothermal reservoir - implications for exploitation (Southern Permian Basin, NE Germany). *Proceedings World Geothermal Congress 2005*, Antalya, Turkey, 24–29 April 2005, 1–5.

Krings, T.: The influence of robust statistics, remote reference, and a criterion based on horizontal magnetic transfer functions on MT data processing. Diploma Thesis, (2007), WWU Münster – GFZ Potsdam. 108 pp.

Moeck, I., Schandlmeier, H. and Holl, H.G.: The stress regime in Rotliegend reservoir reservoir of the Northeast German Basin. *Int. J. Earth Sci. (Geol. Rundsch.)*, (2008), doi:10.1007/s00531-008-0316-1.

Ritter, O., Junge, A. and Dawes, G.: New equipment and processing for magnetotelluric remote reference processing, *Geophys. J. Int.*, **132**, (1998), 535–548.

Rodi, W. and Mackie, R.L.: Nonlinear conjugate gradients algorithm for 2-D magnetotelluric inversions. *Geophysics*. **66**, (2001), 174-187.

Weckmann, U., Magunia, A. and Ritter, O.: Effective noise separation for magnetotelluric single site data processing using a frequency domain selection scheme, *Geophys. J. Int.*, **161**, (2005), 456–468.